

Structure and stability of nitrogen hydrate in a single-walled carbon nanotube under external electric fields

Chi Xu(徐驰), Jiaxian Li(厉嘉贤), Min Wei(韦敏), Xiaoyan Zhou(周晓艳), and Hangjun Lu(陆杭军)
Citation: Chin. Phys. B, 2023, 32 (**7**): 076402. DOI: 10.1088/1674-1056/accd4a
Journal homepage: http://cpb.iphy.ac.cn; http://iopscience.iop.org/cpb

What follows is a list of articles you may be interested in

Anion type-dependent confinement effect on glass transitions of solutions of LiTFSI and LiFSI

Jinbing Zhang(张晋兵), Fengping Wang(王凤平), Zexian Cao(曹则贤), and Qiang Wang(王强)
Chin. Phys. B, 2023, 32 (**7**): 076401. DOI: 10.1088/1674-1056/acca0d

Spatial distribution order parameter prediction of collective system using graph network

Huimin Zhao(赵慧敏), Rui Wang(王瑞), Cai Zhao(赵偲), and Wen Zheng(郑文)
Chin. Phys. B, 2023, 32 (**5**): 056402. DOI: 10.1088/1674-1056/acb9fa

Stability of the topological quantum critical point between multi-Weyl semimetal and band insulator

Zhao-Kun Yang(杨兆昆), Jing-Rong Wang(王景荣), and Guo-Zhu Liu(刘国柱)
Chin. Phys. B, 2023, 32 (**5**): 056401. DOI: 10.1088/1674-1056/acbaf2

Investigation of spatial structure and sympathetic cooling in the $^{9}Be^{+}$–$^{40}Ca^{+}$ bi-component Coulomb crystals

Min Li(李敏), Yong Zhang(张勇), Qian-Yu Zhang(张乾煜), Wen-Li Bai(白文丽), Sheng-Guo He(何胜国), Wen-Cui Peng(彭文翠), and Xin Tong(童昕)
Chin. Phys. B, 2023, 32 (**3**): 036402. DOI: 10.1088/1674-1056/ac70b2

Structure and stability of nitrogen hydrate in a single-walled carbon nanotube under external electric fields

Chi Xu(徐驰), Jiaxian Li(厉嘉贤), Min Wei(韦敏), Xiaoyan Zhou(周晓艳)[†], and Hangjun Lu(陆杭军)[‡]

Department of Physics, Zhejiang Normal University, Jinhua 321004, *China*

(Received 10 February 2023; revised manuscript received 19 March 2023; accepted manuscript online 16 April 2023)

The effects of an external electric field on the structure and stability of the nitrogen hydrate confined in a single-walled carbon nanotube (CNT) were studied by using molecular dynamics (MD) simulations. It was found that the structure of the nitrogen hydrate, the occupancy and distribution of the nitrogen molecules inside the nanotube depend sensitively on the direction of the external electric field. A parallel electric field can destabilize the nitrogen hydrate and cause the release of nitrogen molecules from the ice nanotube of the hydrate. While a vertical electric field can redistribute the nitrogen molecules from the core to the shell of the hydrate. The occupancy of the nitrogen molecules of the hydrate follows a sigmoid-like function as the direction of the electric field changes. Our findings may aid in the development of methods to control gas release and encapsulation by using electric fields.

Keywords: nitrogen hydrate, ice nanotube, electric field

PACS: 64.70.F–, 68.03.Hj, 68.03.–g, 68.18.Jk **DOI:** 10.1088/1674-1056/accd4a

1. Introduction

Gas hydrate has elicited great research interest due to the broad prospect of use in industrial applications, including gas storage,[1–4] gas transportation, gas separation and energy carrier.[5–10] Gas hydrates are a class of crystalline compounds composed of ice-like cages formed by water molecules and gas molecules trapped inside these cages. It has been recognized that there are three conventional crystalline structures (sI, sII, and sH) of gas hydrate in the bulk.[11–13] Though gas hydrates exist naturally in large quantities on the ocean floor and permafrost regions. It is found that the formation of gas hydrates in bulk is not easy and requires extreme conditions.[14]

Significant researches have been devoted to understand the formation of gas hydrate and to ameliorate the extreme pressure and temperature for forming gas hydrates.[15–18] It has been confirmed that porous materials can promote the nucleation of gas hydrate due to their high surface area and specific surface properties.[19–22] The confinement effects of nanosized pores on the growth of gas hydrates have been investigated widely.[23–25] The unique phase behavior of water confined in nanosized space originates from the hydrogen bonding interactions and spatial inhomogeneity which significantly affects the growth kinetics of gas hydrates.[26,27] Therefore, the structures and thermodynamic phase behavior of the gas hydrates is sensitive to the properties of the surface and the size of pores in porous materials.

When the pore size is reduced to subnanometer, the structures and kinetics of gas hydrates show different characteristics due to the highly confined environment. In two-dimensional (2D) nanoconfinement, Zeng's group provided the first simulation evidence of the spontaneous formation of 2D monolayer argon hydrate within hydrophobic nanoslit in 2010.[28] Many new 2D gas hydrates trap different gas such as H_2, CH_4, and CO_2 within hydrophobic slit nanopores have been revealed using MD simulations or density functional theory calculations.[29–32] CNTs are ideal "one-dimensional (1D) pores", which have been explored to provide 1D channels for growing gas hydrates. In 2005, Tanaka and Koga reported the first simulation evidence of the spontaneous formation of a quasi-one-dimensional (Q1D) gas hydrate in CNTs.[33] It is made of an octagonal ice nanotube and a gas molecules wire (such as neon, argon, and methane) sitting in the core region. Inspired by this work, Zhao *et al.* found the rapid growth of Q1D H_2 hydrates inside CNTs at near ambient temperature and pressure.[34] They further demonstrated the selectivity of CO or CO_2 via the formation of Q1D polygonal gas hydrates within CNTs, which can be exploited for hydrogen purification in full cells.[9,35] The formation of CH_4 hydrates in CNTs with different sizes was reported by Akbarzadeh *et al.* using MD simulations.[36] Their results revealed that, unlike the other gas hydrates, the methane molecules replace some of the water molecules in the polygonal ice nanotube and the replaced water molecules occupy the central hollow space.

Though numerous articles have reported the spontaneous growth and structures of low-dimension gas hydrates in highly confinement spaces, it is still difficult to control the growth and release processes. CNTs are promising for a storage medium for gas hydrates due to their high strength, stability, and small size. The unique properties of CNTs allow

[†]Corresponding author. E-mail: zxylu@zjnu.cn
[‡]Corresponding author. E-mail: zjlhun@zjnu.cn

© 2023 Chinese Physical Society and IOP Publishing Ltd

for high storage density and efficient storage and release of gases. Hence, developing new approaches to control gas encapsulation as well as gas release is important and necessary. It has been recognized that electric field is an effective and convenience way to modify the interfacial properties of water at the nanoscale.[37–40] A number of studies demonstrated that electric field can cause the phase transition of water confined in nanoscale space in recent years.[41,42] Winarto *et al.* demonstrated that the application of an axial electric field can effectively separate different solutions, such as water–ethanol, water–methanol, or methanol–ethanol, using CNTs as a medium.[43,44] Recently, we found that the nitrogen molecules can be released from the gas hydrate in the CNT triggered by axial electric field.[45]

In our study, we utilize MD simulations to examine the impact of an external electric field on the structure and stability of nitrogen gas hydrates inside the CNT. The direction of the electric field is varied, ranging from being parallel to the axis of the CNT to being orthogonal to it. A parallel electric field fixed can destabilize the nitrogen hydrate and cause nitrogen release, while a vertical field can redistribute the molecules from the core to the shell. The occupancy of nitrogen molecules in the hydrate follows a sigmoidal function as the direction of the electric field changes.

2. Methodology

The simulation framework is illustrated in Fig. 1. The simulation box contains an uncapped (10,10) CNT of length 10 nm along in z direction and 35 nitrogen molecules are randomly inserted inside the CNT. To improve simulation efficiency and save time, we randomly introduced nitrogen molecules into the CNT for this project. The whole system is solvated with 4212 TIP4P water molecules.[46] All MD simulations are performed using the GROMACS simulation package 2018.3 in the NPT ensemble.[47] An isotropous pressure of 150 MPa is applied by using Parrinello–Rahman algorithm.[48] Constant temperature (240 K) is maintained by using a V-rescale thermostat with $\tau = 0.1$ ps.[49] And periodic boundary conditions are applied in all directions. In the present work, the carbon atoms in the CNT and the nitrogen atoms are modeled as uncharged Lennard–Jones (LJ) particles with parameters: $\sigma_{CC} = 0.34$ nm, $\varepsilon_{cc} = 0.3612$ kJ/mol, $\sigma_{NN} = 0.3256$ nm, and $\varepsilon_{NN} = 0.2888$ kJ/mol. The N–N interatomic distance is 0.14 nm, maintained by harmonic potentials with a spring constant of 1.280×10^6 kJ/mol·nm^2, which is the same as the parameters used in previous studies.[50–52] The LJ interactions are calculated using Lorentz–Berthelot combination rules. The short-range van der Waals forces had a cutoff distance of 1.4 nm. The longrange electrostatic forces are calculated using the particle-mesh Ewald method with a cutoff for real space of 1.4 nm. The time step is 1 fs.

After 100-ns simulation, a Q1D nitrogen gas hydrate is formed spontaneously and well equilibrated (Fig. 1). During the simulations, the carbon atoms of the SWNT are kept fixed at the original positions. Then we started all other simulations with this equilibrated system. Different from the previous work in which axial electric fields were employed.[43,44] Here, two external electric fields in the x and z directions (E_x and E_y) are applied to create an electric field E with a constant strength of 1.75 V/nm. Based on our previous research,[45] at this strength, water–electric field interaction is equivalent to the potential energy of water molecules in CNTs. The direction of the electric field E is denoted by the angle α (as shown in Fig. 3(a)). The MD simulations with different E_x and E_y (*i.e.*, different α, $0^\circ \leq \alpha \leq 90^\circ$) are performed. The simulation time for each case is larger than 100 ns, and the last 100 ps of the simulations is collected for analysis.

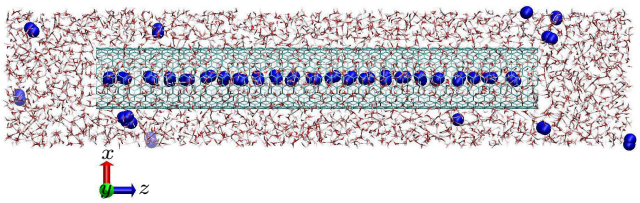


Fig. 1. Side views of the simulation framework generated using VMD. Cyan lines and blue spheres represent the single-wall CNT and atoms of nitrogen molecules, respectively. Water molecules are indicated by red lines.

3. Results and discussion

Initially, in the absence of electric field, a perfect Q1D nitrogen gas hydrate can self-assemble within the CNT. The water molecules arrange themselves into an octagonal ice nanotube with a nitrogen wire located in its central region, as shown in Fig. 1. This result is in agreement with previous research findings.[33,34,45] The number of nitrogen molecules within the CNT is about 23.

In order to explore the effect of external electric field on the structure and stability of the nitrogen hydrate, we have simulated the behavior of nitrogen molecules and water inside the CNT under electric fields ($E = 1.75$ V/nm) with different directions. First, we calculated the number of nitrogen molecules and water molecules remaining inside the CNT after the system reaches equilibrium for each case, as shown in Fig. 2. The angle α is the direction of the electric field and is defined as the angle between the direction of the total electric field $\boldsymbol{E}$ and the z axis in the z–x plane. When an electric field is introduced and $\alpha \leq 24^\circ$, all nitrogen molecules are released from the nitrogen hydrate within the CNT and enter into the reservoirs. As a result, the number of nitrogen molecules, N_{N2}, remaining within the CNT becomes zero, while the number of water molecules, N_{H_2O}, within the CNT, increases from

281 to 306. As the angle of the electric field increases within the range of $24^\circ < \alpha < 62^\circ$, there is a noticeable increase in the number of nitrogen molecules remaining within the CNT. We note that, as α is close to 45°, the number of nitrogen molecules as well as the water molecules exhibits large fluctuations. In the range of $62^\circ \leq \alpha \leq 90^\circ$, the majority of nitrogen molecules remain within the CNT despite the presence of an electric field. The number of nitrogen molecules approaches ~ 23, which is equal to the number of the nitrogen molecules in the nitrogen wire in the initial state (Fig. 1). The number of water molecules remaining within the CNT with α is shown in Fig. 2(b). It is evident that the field-direction dependence of the water occupancy is inversely correlated with the nitrogen occupancy. Additionally, the results show that the occupancy of water molecules within the CNT increases with E_z increasing as reported by Winarto.[37]

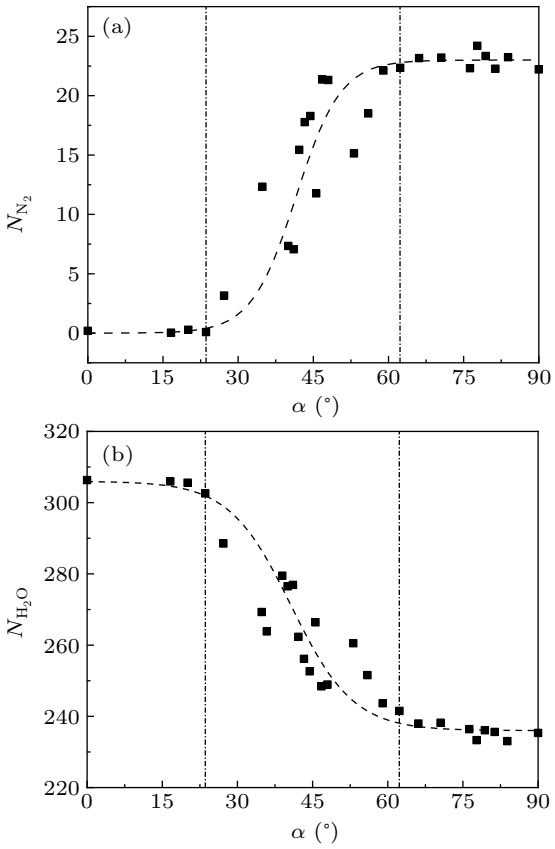


Fig. 2. The influence of electric field orientation on the nitrogen hydrate. The number of nitrogen molecules (a) and water molecules (b) remaining in CNT after the system reaches equilibrium as a function of the angle α, where α is the angle formed between the electric field $\boldsymbol{E}$ and the z direction.

Then, we examine the changes in the structures of the nitrogen hydrate. Figure 3(a) shows the snapshots for some typical states (initial state, and $\alpha = 0^\circ$, 45°, 90°). To discuss the characteristics of the ice nanotubes, we unwrap the ice nanotube onto the 2D surface (the $\boldsymbol{e}_t$–$\boldsymbol{e}_z$ plane) as shown in Fig. 3(b), and introduce a parameter β, where β is the angle formed between the hydrogen bond of the ice nanotube and the z direction as depicted in Figs. 3(c)–3(d). Comparing the initial state ($E = 0$) with that for $\alpha = 0^\circ$ in Fig. 3(a), we observed that the nitrogen molecules were released from the octagonal ice nanotube and displaced by a water chain. This process also causes a structural transition of the ice nanotube, from an octagonal to a helical structure, as evidenced by the unwrapped ice nanotube in Figs. 3(c)–3(d). In the cases of $\alpha = 45^\circ$, we observed that the external electric field disturbed the hydrogen bonding network, leading to the formation of defects on the helical structure (see Fig. 3(e)). Additionally, some nitrogen molecules failed to be expelled from the ice nanotube, becoming embedded in the ice shell. When the electric field turns to perpendicular to the nanotube ($\alpha = 90^\circ$), almost all of the nitrogen molecules remain within the CNT. At the same time, the structure of the ice nanotube undergoes a significant transformation, with the nitrogen molecules moving from the core to the wall of the ice nanotube and the core region being occupied by a water chain. Similar hydrate structures were observed by Akbarzadeh *et al.*, in their results, methane molecules were located in the wall of the ice nanotube in (14,0) or (15,0) CNT in the absence of electric field. This structure is a result of two factors: the disruption of hydrogen bonds induced by the electric field and the strong LJ attraction interaction between the nitrogen molecules and the CNT. Thus, under a parallel electric field, the water molecules have a higher preference to enter the CNT compared to the nitrogen molecules, while under an orthogonal electric field, the nitrogen molecules have a higher preference to remain inside the nanotube compared to the water molecules.

We also studied the structural characteristics of the clathrate by analyzing the probability distribution of the angle β as shown in Fig. 3(g). In the initial case ($E = 0$ V/nm), two peaks were observed, at $\beta = 10^\circ$ and $\beta = 80^\circ$, representing two distinct orientations of the water chains of the ice nanotube as depicted in Fig. 3(c). When $\beta = 10^\circ$, the direction of a typical type of hydrogen bond in a water chain is almost aligned with the z axis. And, for $\beta = 80^\circ$, the direction corresponds to another type of hydrogen bond that is almost perpendicular to the z axis (along the $\boldsymbol{e}_t$). Surprisingly, the distribution of β is not symmetrical, even though ice nanotubes appear to be structurally symmetrical. The peak value at $\beta = 80^\circ$ is significantly larger than the peak value at $\beta = 10^\circ$. This is due to the asymmetry caused by confinement. The hydrogen bonds of the octagonal water molecule rings that form the ice nanotube are more stable in the radial direction due to confinement (corresponding to $\beta = 80^\circ$), while the hydrogen bonds linking each octagonal molecule ring (corresponding to $\beta = 10^\circ$) are not confined in the z direction, leading to the possibility of local breakage due to the motion of the ice nanotube in the z direction. When an electric field of $E = 1.75$ V/nm

is applied parallel to the z axis ($\alpha = 0°$), the peak at $\beta = 80°$ is shifted to $\beta = 63°$ and the peak at $\beta = 10°$ is noticeably reduced and is broadened. The shift of the peaks reflects the structure transition of the ice nanotube from octagonal ice nanotube to helical structure (see Figs. 3(a)–3(b)). As the angle α increases to 27.2°, the peak value significantly decreases, indicating that the orientation of water molecule chains tends towards disorder, which is related to the breakage of hydrogen bond networks and the formation of defects, as shown in Figs. 3(e)–3(f). When the electric field is perpendicular to the CNT ($\alpha = 90°$), there is no obvious peak in the β distribution profile. The nitrogen molecules that remain within the CNT are displaced from the core to the shell of the ice nanotube, disrupting the hydrogen bond network and causing a decline in the long-range structural order of the system, corresponding to the structures shown in Figs. 3(e)–3(f). The red dashed circles indicate the locations of the nitrogen molecules in the ice nanotube shell.

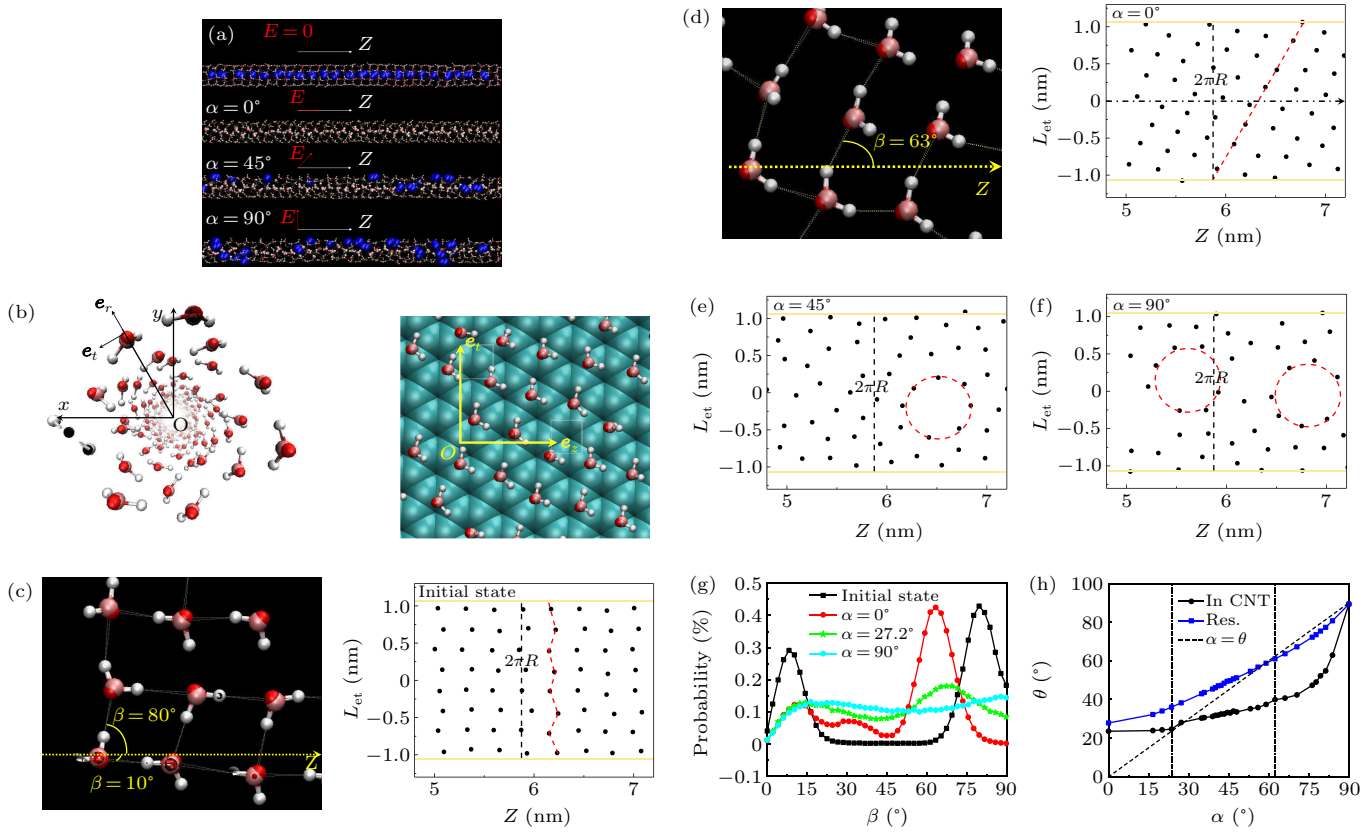


Fig. 3. The influence of electric field orientation on the structure of nitrogen hydrate. (a) Illustrating the side views of the structures of water molecules and the distributions of the nitrogen molecules inside the CNT at four representative scenarios. (b) Snapshot of the helical ice nanotube for the electric field aligned with z axis ($\alpha = 0°$) and a scheme for unwrapped ice nanotube and the CNT into a 2D plane (right). (c)–(f) The 2D surface by unwrapping the ice nanotube. And the schematic diagram of the angle β. The red dash circles represent the defects on the ice nanotube shell. (g) The probability distribution of the angle β for typical cases. (h) The angle θ between the water molecule dipole and z axis *versus* the direction of electric field α.

Furthermore, we analyzed the angle θ between the water dipole and the z axis, as shown in Fig. 3(h). For bulk water, the water molecule dipoles tend to align with the electric field due to the strong electric interaction. As a result, the average angle θ of the bulk water increases linearly with the direction of the electric field α. However, for the water molecules within the clathrate inside the CNT, the average θ remains almost unchanged for $0° \leq \alpha \leq 24°$. As the direction of the electric field enters the range of $24° < \alpha < 70°$, the average θ increases gradually with increasing angle α. Interestingly, with further increases in α, the average angle θ rapidly increases from 50° to 90°. The response of water dipoles to an external electric field varies greatly between bulk and confined water molecules within CNTs. In bulk, water molecules exist in a liquid state, whereas in CNTs, they can form clathrate hydrate structures and become confined to a crystalline arrangement within the nanotube when the angle α is between 0° and 24°. This confinement results in a different behavior of the water molecules, affecting their response to external stimuli.

The structure and phase of water inside CNTs are highly dissimilar when exposed to parallel and vertical electric fields. The diffusion coefficient of water molecules within the CNT significantly increases from 2.1×10^{-8} cm^2·s^{-1} to 7.0×10^{-6} cm^2·s^{-1} as α increases from 0° to 90°. Parallel electric fields cause the water molecules to form helical hydrate structures and become confined in a crystalline arrangement, whereas vertical electric fields result in the loose structure of the ice nanotube. This distinct behavior of water within CNTs

is attributed to the orientation and confinement of the water molecules, leading to varying responses to external stimuli.

To clarify the distribution of N_2 molecules on the shell of the ice nanotube, we calculated 2D radial probability density distribution of the nitrogen molecules averaged over the last 20 ns, the results are shown in Fig. 4. In the field-free case, all of the nitrogen molecules stay in the core region of the ice nanotube, leading to a peak in the 2D radial nitrogen distribution as shown in Fig. 4(a). When a parallel electric field $E = 1.75$ V/nm is applied ($\alpha = 0°$), there is no nitrogen molecules within the CNT. As $\alpha = 45°$, the density distribution of nitrogen molecules is not angularly symmetrical and there is a highdensity region in the vicinity of 90°, suggesting that nitrogen molecules prefer to stay on the top region (see Fig. 4(c)). When α further increases to 90° (*i.e.*, orthogonal electric field), the density distribution of N_2 molecules exhibits left-right symmetry. The likelihood of N_2 molecules residing in the upper region of the interior surface of the nanotube is higher compared to the lower region. From the preceding discussion, it can be inferred that the orthogonal component of the electric field is favorable for N_2 molecules to remain within the nanotube. Moreover, the arrangement of N_2 molecules on the surface of the nanotube is highly sensitive to the direction of the electric field.

In order to explore the cause of the non-uniform distribution of nitrogen molecules, we analyze the structure and orientation of the hydrogen bond network. Firstly, the ice shell is divided into four regions, labeled as top, bottom, left, and right, as shown in Fig. 5(a). We calculated the number of hydrogen bonds (H bonds) formed by a water molecule with its neighboring water molecules in each region, and the results are shown in Fig. 5(b). When the electric field is parallel to the axis of the nanotube ($\alpha = 0°$), the average number of H bonds per water molecule is the same across all four regions, as expected. However, when α increases, the component E_x disrupts the symmetry of the hydrogen bond network. The average number of H bonds in the bottom region remains almost unchanged, while the top region sees a significant decrease, dropping from 1.02 to 0.76 when α increases to 90°. The asymmetry in the number of hydrogen bonds caused by the direction of the electric field along the normal or negative direction of the hydrophobic surface has also been observed in our previous work.[53] The left and right regions also experience a decrease in the average number of H bonds. The interruption of H bonds leads to defects in the top, left, and right regions of the ice shell, making it more likely for nitrogen molecules to stay in these regions. The variance in the average number of H bonds between the top and bottom regions, caused by the influence of an external electric field, leads to an uneven distribution of nitrogen molecules.

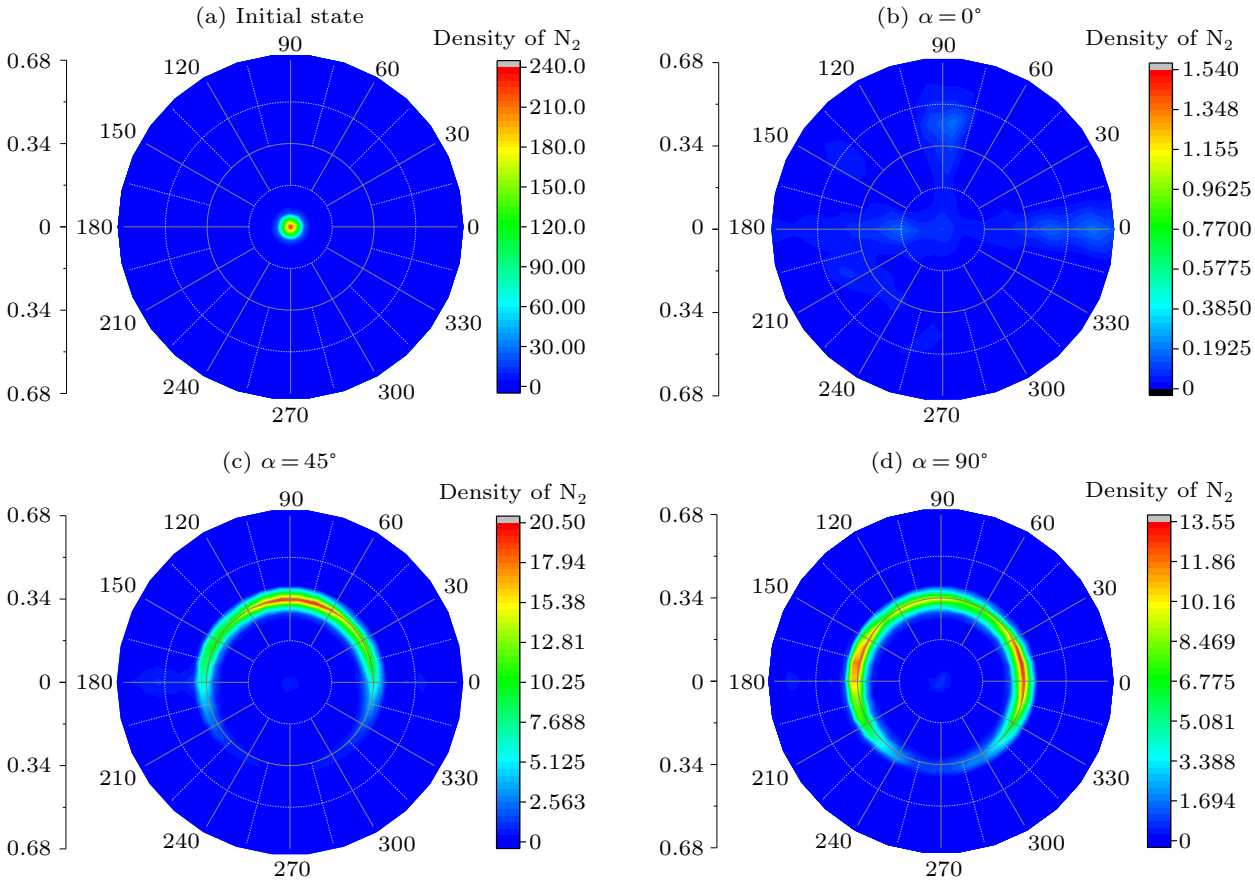


Fig. 4. The 2D radial distribution plots of the nitrogen molecules inside CNT under different electric fields.

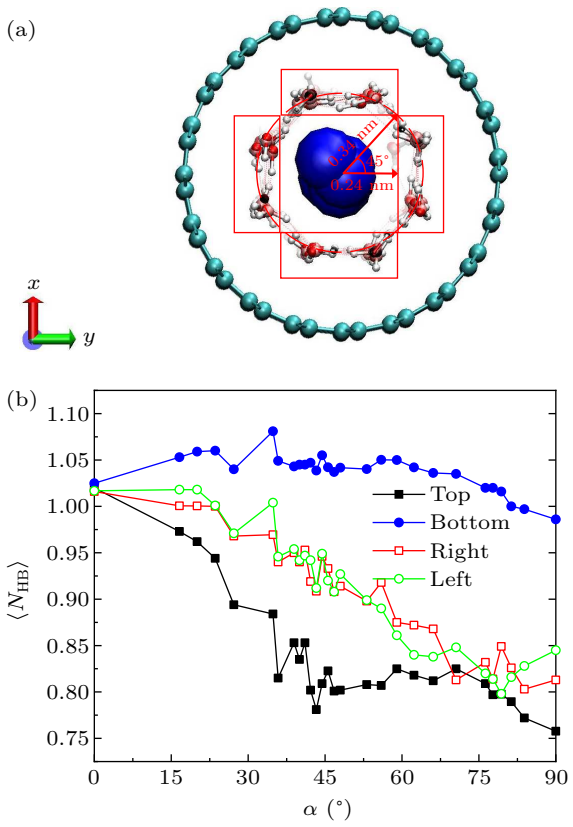


Fig. 5. (a) The schematic of the divisions of the ice shell: top, bottom, left and right regions, each with a central angle of 90°. (b) Average number of hydrogen bonds formed by a water molecule with other water molecules within the same region as a function of the angle α.

4. Conclusion

In this study, we investigated the impact of an external electric field on the structure and stability of nitrogen hydrates in the CNT. Without external electric field, a Q1D nitrogen hydrate with nitrogen molecules aligned in the core region of the ice nanotube can be formed spontaneously in the CNT. Applying an electric field of sufficient strength along the axis of the CNT can destabilize the Q1D nitrogen hydrate. This results in the release of nitrogen molecules from the ice nanotube and a structure transition of the ice nanotube from octagonal to helical. When a vertical electric field is applied, almost all of nitrogen molecules remain within the CNT, causing the structure to become less compact as nitrogen molecules redistribute from the core to the shell of the ice nanotube. As the angle (α) between the direction of the electric field and the z axis (the axis of the CNT) increases in the range of 0°–90°, the occupancy of the nitrogen molecules of the hydrate follows a sigmoid-like function and increases accordingly. Furthermore, the distribution of nitrogen molecules on the wall of the ice nanotube is uneven due to the strong response of the hydrogen bonds connecting water molecules in the ice nanotube to external electric fields. More hydrogen bonds are broken in the top, left, and right regions, causing nitrogen molecules to preferentially reside there. Our findings may aid in the development of methods to control gas release and encapsulation by using electric fields.

Acknowledgment

Project supported by the National Natural Science Foundation of China (Grant No. 11875237).

References

[1] Veluswamy H P, Kumar A, Seo Y, Lee J D and Linga P 2018 *Appl. Energ.* **216** 262
[2] Mao W L and Mao H K 2004 *Proc. Natl. Acad. Sci. USA* **101** 708
[3] Lee H L J W, Kim D Y, *et al.* 2005 *Nature* **434** 743
[4] Florusse L J, Peters C J, Schoonman J, Hester K C, Koh C A, Dec S F, March K N and Sloan E D 2004 *Science* **306** 469
[5] Englezos P and Lee J D 2005 *Korean J. Chem. Eng.* **22** 671
[6] Babu P, Linga P, Kumar R and Englezos P 2015 *Energy* **85** 261
[7] Xu C G and Li X S 2014 *Rsc. Advances* **4** 18301
[8] Struzhkin V V, Militzer B, Mao W L, Mao H K and Hemley R J 2007 *Chem. Rev.* **107** 4133
[9] Zhao W, Francisco J S and Xiao C Z 2016 *J. Chem. Phys. Lett.* **7** 4911
[10] Yu X H, Liu Y, Du S Y, Zheng X, Zhu J L, Xu H W, Zhang J Z, Du S Y, Zeng X C and Francisco J 2020 *Chin. Phys. Lett.* **37** 048201
[11] McMullan R K and Jeffrey G 1965 *J. Chem. Phys.* **42** 2725
[12] Mak T C and McMullan R K 1965 *J. Chem. Phys.* **42** 2732
[13] Ripmeester J A, Tse J S, Ratcliffe C I and Powell B M 1987 *Nature* **325** 135
[14] Mao W L, Mao H K, Goncharov A F, Struzhkin V V, Guo Q, Hu J, Shu J, Hemley R J, Somayazulu M and Zhao Y 2002 *Science* **297** 2247
[15] Casco M E, Silvestre-Albero J, Ramírez-Cuesta A J, Rey F, Jordá J L, Bansode A, Urakawa A, Peral I, Martínez-Escandell M and Kaneko K 2015 *Nat. Commun.* **6** 6432
[16] Miyawaki J, Kanda T, Suzuki T, Okui T, Maeda Y and Kaneko K 1998 *J. Phys. Chem. B* **102** 2187
[17] Borchardt L, Nickel W, Casco M, Senkovska I, Bon V, Wallacher D, Grimm N, Krause S and Silvestre-Albero J 2016 *Phys. Chem. Chem. Phys.* **18** 20607
[18] Guo P, Qiu Y L, Li L L, Luo Q, Zhao J F and Pan Y K 2018 *Chin. Phys. B* **27** 043103
[19] Buffett B and Zatsepina O Y 2000 *Mar. Geol.* **164** 69
[20] Prasad P S, Sowjanya Y and Dhanunjana Chari V 2014 *J. Phys. Chem. C* **118** 7759
[21] Linga P, Haligva C, Nam S C, Ripmeester J A and Englezos P 2009 *Energ. Fuel* **23** 5496
[22] Kumar K V, Preuss K, Titirici M M and Rodríguez-Reinoso F 2017 *Chem. Rev.* **117** 1796
[23] Byl O, Liu J C, Wang Y, Yim W L, Johnson J K and Yates J T 2006 *J. Am. Chem. Soc.* **128** 12090
[24] Kolesnikov A I, Zanotti J M, Loong C K, Thiyagarajan P, Moravsky A P, Loutfy R O and Burnham C J 2004 *Phys. Rev. Lett.* **93** 035503
[25] Borchardt L, Casco M E and Silvestre-Albero J 2018 *Chem. Phys. Chem.* **19** 1298
[26] Khurana M, Yin Z and Linga P 2017 *ACS Sustainable Chemistry & Engineering* **5** 11176
[27] Bai D, Chen G, Zhang X and Wang W 2011 *Langmuir* **27** 5961
[28] Bai J, Angell C A and Zeng X C 2010 *Proc. Natl. Acad. Sci. USA* **107** 5718
[29] Zhao W H, Wang L, Bai J, Yuan L F, Yang J and Zeng X C 2014 *Acc. Chem. Res.* **47** 2505
[30] Zhao W H, Bai J, Wang L, Yuan L F, Yang J, Francisco J S and Zeng X C 2015 *J. Mater. Chem. A* **3** 5547
[31] Bai J and Zeng X C 2012 *Proc. Natl. Acad. Sci. USA* **109** 21240
[32] Zhong H, Li L, Ma R, Zhong J, Yan Y, Li S, Zhang J and Liu J 2020 *Phys. Chem. Chem. Phys.* **22** 5774
[33] Tanaka H and Koga K 2005 *J. Chem. Phys.* **123** 094706
[34] Zhao W, Wang L, Bai J, Francisco J S and Zeng X C 2014 *J. Am. Chem. Soc.* **136** 10661
[35] Zhao W, Bai J, Francisco J S and Zeng X C 2018 *J. Phys. Chem. C* **122** 7951
[36] Akbarzadeh H, Abbaspour M, Salemi S and Nazarian A 2018 *New J. Chem.* **42** 7083

[37] Winarto, Takaiwa D, Yamamoto E and Yasuoka K 2015 *J. Chem. Phys.* **142** 124701
[38] Mei F, Zhou X, Kou J, Wu F, Wang C and Lu H 2015 *J. Chem. Phys.* **142** 134704
[39] Vaitheeswaran S, Yin H and Rasaiah J C 2005 *J. Phys. Chem. B* **109** 6629
[40] Vaitheeswaran S, Rasaiah J C and Hummer G 2004 *J. Chem. Phys.* **121** 7955
[41] Fu Z, Luo Y, Ma J and Wei G 2011 *J. Chem. Phys.* **134** 154507
[42] Kayal A and Chandra A 2015 *J. Chem. Phys.* **143** 224708
[43] Winarto, Takaiwa D, Yamamoto E and Yasuoka K 2016 *Phys. Chem. Chem. Phys.* **18** 33310
[44] Winarto, Takaiwa D, Yamamoto E and Yasuoka K 2015 *Nanoscale* **7** 12659
[45] Li J, Lu H and Zhou X 2020 *Nanoscale* **12** 12801
[46] Jorgensen W L, Chandrasekhar J, Madura J D, Impey R W and Klein M L 1983 *J. Chem. Phys.* **79** 926
[47] Hess B, Kutzner C, Van Der Spoel D and Lindahl E 2008 *J. Chem. Theory Comput.* **4** 435
[48] Parrinello M and Rahman A 1981 *J. Appl. Phys.* **52** 7182
[49] Bussi G, Donadio D and Parrinello M 2007 *J. Chem. Phys.* **126** 014101
[50] Rappé A K, Casewit C J, Colwell K, Goddard III W A and Skiff W M 1992 *J. Am. Chem. Soc.* **114** 10024
[51] Li W, Zuo X, Zhou X and Lu H 2019 *J. Chem. Phys.* **150** 104702
[52] Zhang M, Zuo G, Chen J, Gao Y and Fang H 2013 *Sci. Rep.* **3** 1660
[53] Feng Q, Li J, Zhou X and Lu H 2022 *Chin. Phys. B* **31** 036801